Available online at www.sciencedirect.com

ScienceDirect

Procedia CIRP 102 (2021) 13–18

www.elsevier.com/locate/procedia

18th CIRP Conference on Modeling of Machining Operations

A Residual Stress Prediction of Machining IN718 Produced by Direct Energy Deposition

Francesco Careri[a], Stano Imbrogno[b]*, Domenico Umbrello[a], José C. Outeiro[c], António C. Batista[d]

[a]Department of Mechanical, Energy and Management Engineering, University of Calabria, Rende, CS 87036, Italy

[b]School of Metallurgy and Materials, University of Birmingham, Birmingham B15 2TT, UK

[c]Arts et Metiers Institute of Technology, LABOMAP, HESAM University, Rue Porte de Paris, F-71250 Cluny, France

[d] Univ Coimbra, CFisUC, Department of Physics, P-3004-516 Coimbra, Portugal

* Corresponding author. Tel.: +44-(0)121-414-7899 ; *E-mail address:* s.imbrogno@bham.ac.uk

Abstract

The paper presents a Finite Element Modelling (FEM) of the turning process on the Nickel superalloy IN718 produced by the Direct Energy Deposition (DED) to predict the residual stress. The material behaviour was implemented by a customized user-routine to take into account the anisotropy of the material due to the DED process. The residual stresses were experimentally measured on the surface and beneath the machined surface and the data collected were used to validate the FEM model.

Keywords: IN718; Direct Energy Deposition; Residual Stress; Finite Element Model

1. Introduction

Nickel-based superalloys have been widely used for application involving severe environment conditions due to their high strength and corrosion resistance during the service above 750°C [1,2]. In particular, IN718 is the most commonly used Nickel-based superalloy to produce components in the aeronautical and aerospace sectors, thanks to the high content of Ni, Cr and Fe [3]. The introduction of Additive Manufacturing (AM) enhanced the design and the quality of the parts produced conventional manufacturing technologies, thanks to its ability to produce very complex parts in a relatively short time and without wasting material. However, additive techniques are not able to guarantee a finished product in a single operation. AM needs traditional machining operations to overcome defects such as poor surface finish and geometric tolerances. Post-processing operations, such as turning or milling, are essential to meet the high-quality standards required in the industrial fields [4]. The IN718 represents a challenging material concerning the machining processes, especially for geometrically complex shapes, due to the severe tool wear and poor surface finish. Moreover, the IN718 is considered a very difficult-to-machine material due to its high mechanical and thermal property, high hardness and low thermal conductivity. Consequently, the AM technique is preferred for the manufacturing process of IN718 components [5,6] Moreover, considering the different behaviour of the additively materials compared to those produced by conventional techniques (e.g. casting, forging), many studies on the influence of mechanical processing on mechanical and microstructural properties, and the surface integrity of components made by AM can be found in the literature [7–9].

10.1016/j.procir.2021.09.003

However, there is a lack of knowledge about on the residual stresses induced by the post-process operations such as machining. The evaluation of the residual stresses is important since they affect the fatigue life and creep resistance. Therefore, the prediction of the residual stress could improve the final qualities of the finished product and therefore improve the fatigue life, fracture behaviour, and corrosion resistance [10]. Considering the cost of the optimization procedures of the machining process, the use of the traditional experimental approach is generally not economically convenient. For this reason, a numerical approach is often used as analysis technique to reduce the relative costs and decrease the range of parameters to be investigated to optimize the manufacturing process [11]. Many numerical models are available for the prediction of residual stresses in the machining of casting IN718 [12–14]. On the other hand, not many works have been published regarding the FEM of machining operations of materials produced through AM processes. This is mainly due to the lack of solid constitutive laws for the AM material behaviour. Indeed, Johnson-Cook's model, and similar models, are unable to correctly represent the anisotropic behaviour of additively materials. Recently, some studies are starting to address this lack. Yuan *et al.* [15] studied the behaviour of IN718 alloy made by Direct Energy Deposition (DED) and built a constitutive model that takes into account the anisotropic nature of the material, as a function of temperature and strain rate. However, no works focused on FEM prediction of residual stresses of material AM has been found. Consequently, this work aims to validate a FEM of turning of IN718 material produced via DED to predict the residual stresses. A subroutine based on a modified model by Yuan *et al.* [15] has been implemented in FEM software.

2. Material and Methods

2.1. Experimental procedure

The processed material was the Nickel-based superalloy IN718 as powder.

Table 1. Chemical composition of the IN718 (powder) and nominal range (%wt.) designed by Standard ASTM [16].

Elements	Measured (%wt.)	ASTM Standard (%wt.)
Ni	52.82	50 − 55
Fe	17.0	11 − 22.4
Cr	19	17 − 21
Nb	3.0	4.8 − 5.5
Ti	0.6	0.7 − 1.2
Al	0.8	0.2 − 0.8
Co	1.0	1.0
Mn	0.35	0.4
C	0.08	0.05

The powder material with a particle size range of 45 to 106 μm was used for the fabrication of cylindric samples. Table 1 reports the chemical analysis (%wt.) of the powder used. The comparison with the composition range designated by the ASTM F3055-14a [16] ensured compliance with the standard powder levels during the manufacturing process phase.

The samples were produced via DED through a TRUMPF TLC 1005 (5axis CNC machine) equipped with a TruDisk 4002 disk laser. The DED process consists of a laser beam and a powder jet that, directed into a substrate, create a melt pool. As a result, the components are realised by consecutive deposition of melted layers. In particular, for the cylindrical bars used in this study, the process parameters set on the DED system were: laser power of 400 W, and a three-jet nozzle powder feeding with a scan speed of 275 mm/min and powder flow rate of 9.8 g/min.

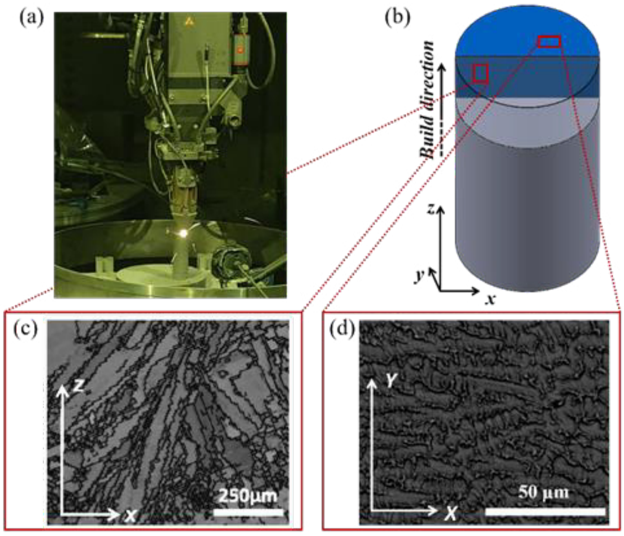

Fig. 1. (a) IN718 sample's DED manufacturing process; (b) Procedure for analysis of microstructure; (c) Microstructure along the build direction; (d) Microstructure along the direction perpendicular to the build direction.

The scan strategy adopted was continuous and rotated of 90° layer by layer. The longitudinal direction of the bar is aligned with the Z build direction. As shown in Fig. 1 (b) and (c) the as-deposited material was characterised by a dendritic microstructure, with element segregations within the dendrites. During the DED process, the heat flow direction was approximately perpendicular to the surface of the substrate or the pre-deposited layers. Consequently, elongated coarse grains have been formed, passing through numerous deposit layer. Majority of the precipitated particles lying adjacent to or along the intergranular regions are identified as Laves phase, rich in Nb, Mo, and Ti and carbide, normally Ti and Nb segregations [17,18]. The as-deposited IN718 shows anisotropic mechanical properties, thanks to the dendritic nature of the microstructure. Furthermore, the build direction affects the tensile and compressive behaviour of the material. This anisotropy is due to the morphology of the columnar grains. Indeed, the dendritic grains are characterized by different sizes along the directions perpendicular to the columnar grains concerning the parallel directions [19].

After the additive process, the cylindrical bars were machined, using two different cutting parameters. In particular, the depth of cut and the feed rate were kept constants and were respectively a_p=0.5 mm and f=0.2 mm/rev. Two different cutting speeds were evaluated, one suggested by the manufacturer of the tools and the second set in order to consider high cutting speeds. Subsequently, some samples were collected by the machined bars to evaluate the effects of the different cutting parameters in terms of the residual stresses beneath the machined surface.

The residual stresses (RS) were analysed on the surface and the subsurface of the samples using an X-ray diffraction technique. Combined with a layer-removal technique the XRD method can generate a residual stress in-depth profile of the material. In this way, all the residual stress history of the material due to a machining process, as such turning, can be evaluated and analysed [20].

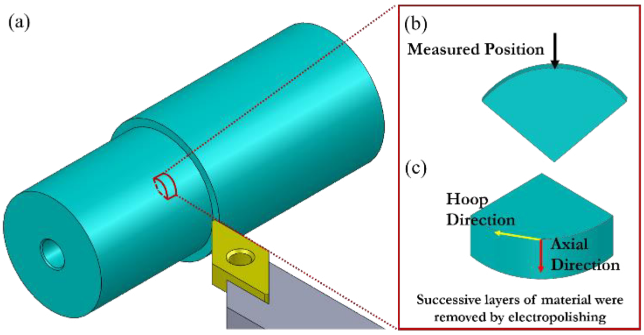

Fig. 2. (a) Area of sample for Residual Stresses measurements; (b) Measurement position for each sample; (c) Directions of Residual Stresses measurements.

As reported in Fig. 2 (c) the residual stresses were determined in both principal directions, the primary motion, hoop direction, and in the feed motion, axial direction. X-ray Mn-Kα radiation was used to determine elastic strains in the {311} diffraction planes (2θ≈152°) of the crystallographic structure of the IN718 alloy, using 22 ψ angles in the range ±44°. Successive layers of material were removed in order to determine the residual stress profiles in depth, avoiding the reintroduction of further residual stresses. Therefore, it was possible to measure the biaxial stresses through the X-ray procedure, with sufficient precision. Further details of the experimental procedures used and results are reported in [21].

2.2. Material constitutive model

A material constitutive model, based on Yuan *et al.* [15], is proposed to define the anisotropic mechanical behaviour of the as-deposited IN718 during machining process. The choice of this constitutive law, instead of the well-known Johnson-Cook's model, is mainly related to the anisotropy incorporated in the model. The constitutive models (e.g. Johnson-Cook) normally used to predict the main variables of the cutting process are not able to describe the thermo-mechanical behaviour of the materials produced by AM. Indeed, Yuan *et al.* considered the state of the material as produced by DED and proposed a model that depends on strain rate, strain, and temperature, as well as on variables such as the microstructure. The proposed anisotropic material constitutive model is given by the following equation:

$$\sigma = \bar{\sigma}_G(T,\varepsilon) + \bar{\sigma}_a + \bar{\sigma}^*(\varepsilon,T,\dot{\varepsilon}) \quad (1)$$

where $\bar{\sigma}_G$ is the equivalent anisotropy component, $\bar{\sigma}_a$ the athermal component, and $\bar{\sigma}^*$ the equivalent thermally activated component, T, ε and $\dot{\varepsilon}$ represent the temperature, the equivalent plastic strain and strain rate, respectively. In detail, the three components are described below:

$$\bar{\sigma}_G = C_0 E(T)\phi(\ln\dot{\varepsilon})\rho^{-\frac{1}{2}} \quad (2)$$

$$\bar{\sigma}_a = C_1\varepsilon^n \quad (3)$$

$$\bar{\sigma}^* = C_2\varepsilon^m exp(-C_3T^* + C_4T^*\ln\dot{\varepsilon})\phi(\ln\dot{\varepsilon})K_p \quad (4)$$

These components are expressed in terms of Young's Modulus (depending on the temperature), strain rate, and dimensions of the dendritic grain. For further detail related to the constitutive model, the reader can consult the work of Yuan *et al.* [15].

The principal parameters and variables involved in the empirical model were taken from a previously published work [22]. In the work, the constitutive model was implemented in a FE software via sub-routine in order to predict the cutting forces and temperatures depending on cutting conditions. In addition, a calibration procedure (trial and error) was performed to define the value of the coefficients of friction. It was ended when the average error representative of the average error of the cutting forces and temperatures was lower than 10%. The model was able to predict the principal variables during the cutting process of the as-deposited IN718. Therefore, the same model was used for the prediction of the residual stress after the machining.

2.3. Numerical model and parameters

The proposed 3D cutting model is detailed in Fig. 3. The model was implemented in the FE software SFTC DEFORM 3D via sub-routine.

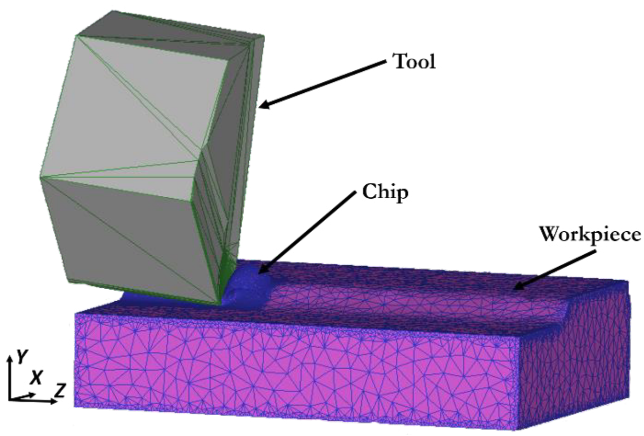

Fig. 3. Objects, geometry and meshing of the FE model.

The workpiece was meshed with 110000 tetrahedral elements and its anisotropic mechanical behaviour was represented by the proposed constitutive model described in the previous section (Eq. 1). A higher density mesh-window was used in the tool-workpiece contact zone, within the workpiece surface, to get more reliable results on the worked surface (minimum element size of 4μm). Moreover, a dynamic local remeshing window was set, following the tool motion, to better predict the stresses and temperatures that occurred during the process. The tool was a CVD multilayer-coated semi-finishing TiAlN insert characterized by rake and clearance angle of 6° and 0°, respectively. The tool geometry and the mechanical behaviour considered are well reported in Careri *et al.* [22]. The tool was meshed with 50000 elements. As done for the workpiece, a finer mesh window was used around the tool nose to better represents the contact in the tool-workpiece working zone. The tool was set-up as a rigid body, while the workpiece considered as an elastoplastic material. This property allowed to take into account the elastic behaviour, responsible of the formation of residual stresses and their variation during the cooling of the workpiece after the turning operation. A hybrid friction model, following a friction law already implemented in the FEM software, was used. A combination of sticking-sliding phenomena that occur into the tool-chip contact region, was employed through two internal coefficients of the model (m and μ). These friction coefficients were found using an iterative analysis aimed to minimize the total average error of predicted cutting forces and temperature, as carried out in the authors' previous work [22]. As reported in the work of Torrano *et al.* [23] the temperature plays a fundamental role in the FE models and at the end of the machining operation, a cooling step must be created.

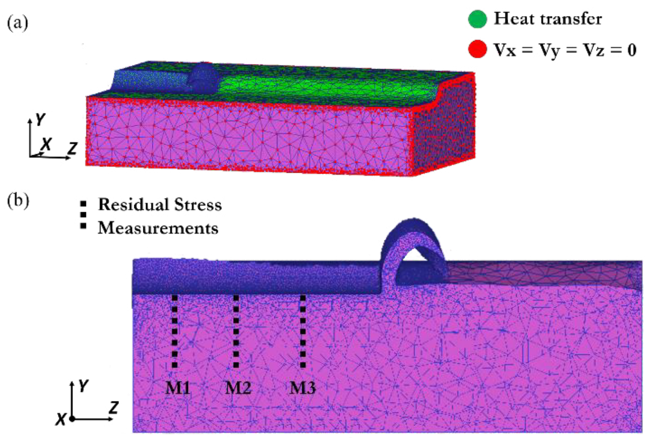

Fig. 4. (a) Separation of the tool from the workpiece; (b) detail of detachment; (c) boundary condition for the cooling process.

Consequently, after the machining simulation, an unloading and cooling step was also considered. A simulation step, where the tool detaches from the workpiece, was created. The tool object was removed once a specific distance is reached, eliminating the contacts between tool and workpiece. New mechanical and thermal boundary conditions were considered, as reported in Fig 4 (a). In particular, the upper and left surface of the workpiece was able to exchange heat with the environment. The convection coefficient of the air, equal to 20 $W/m^2 \cdot K$, was considered during the cooling process. At this point, the evaluation of the residual stresses due to the thermomechanical process was carried out as shown in Fig 4 (b). A procedure proposed by Outeiro *et al.* [24] was applied. In particular, the residual stresses were calculated as the average of 3 measurements carried out on the entire machined layer. The part immediately behind the tool was not considered in the residual stresses measurements because it represented a region where the thermomechanical phenomena did not reach the steady state (especially within the chip formation area).

Table 2 reported the cutting parameters and the levels considered during the experimental campaign. In particular two cutting condition were selected to carry out the prediction of the residual stress from the simulation campaign carried out in the work of Careri *et al.* [22].

Table 2. Cutting condition for experimental and numerical tests.

#Test	Vc [m/min]	f [mm/rev]	a_p [mm]	Cooling Condition
1	70	0.2	0.5	Dry
2	120	0.2	0.5	Dry

3. Results and discussion

To assess the quality of the results predicted by the FE developed model, the cutting forces and the temperature were evaluated and compared with the experimental results. This comparison is well reported, discussed and described in [21]. Therefore, in this work the anisotropic model implemented has been validated for predicting the residual stresses in the turning simulation of IN718.

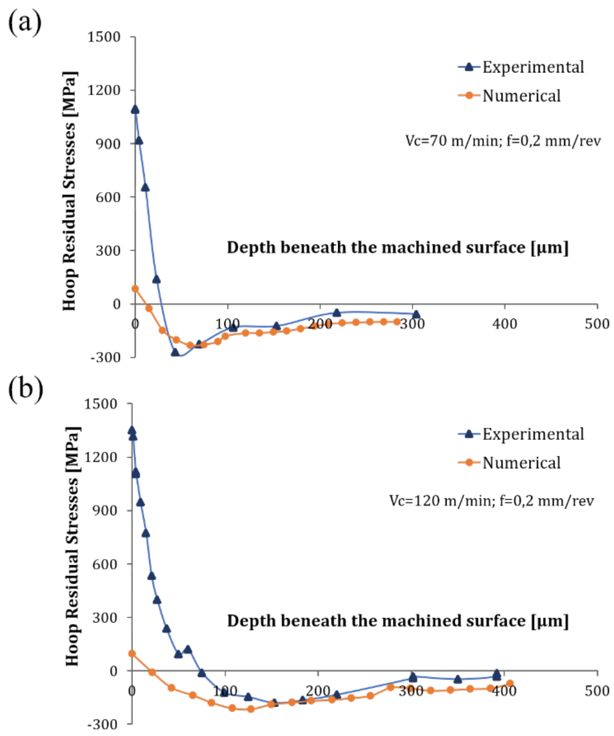

Fig. 5. Comparison of Residual Stress in Hoop Direction for (a) #Test1, Vc=70m/min and f=0.2mm/rev; (b) #Test2, Vc=120m/min and f=0.2mm/rev.

In Fig. 5 (a) and (b) are reported the comparison between experimental and numerical results of the residual stress in hoop direction. In particular, Fig 5 (a) regards the residual stress in hoop direction for the test 1 (Vc=70 m/min; f=0.2 mm/rev). The predicted residual stress was in accordance with the experimental ones measured on the sample. Likewise, also the residual stress in hoop direction for the test 2 (Vc=1200 m/min; f=0.2 mm/rev) was reasonably predicted, considering the variation of the simulated residual stresses beneath the machined surface. The model in both the cases considered was not able to accurately predict the tension values measured immediately under the worked surface (depth less than 50µm).

Concerning the residual stress along the axial direction, reported in Fig. 6 (a) and (b), the predicted residual stress revealed a similar trend in comparison with the experimental ones. On the other hand, the numerical values of the stresses in the axial direction are not perfectly coherent with the experimental measurements (within the 20µm beneath the machine surface). This problem could be related to different issues. First of all, the number of elements used into the cutting zone might led to a lower accuracy in predicting the axial residual stresses. In particular, the mesh size within the 20µm-30µm could be optimised to enhance the values computed to the nodes. A smaller element size is essential to predict with accuracy the high variation in residual stresses measured in a very small portion of material affected by the tool action. An optimised mesh, capable to link the values across nodes, should permit to predict values very close to the experimental ones but, on the other hand, leading to a higher computation time. The second reason can be related to the material constitutive model used in this work. Indeed, although the model used represented the typical anisotropy of materials produced by AM, the plastic flow is activated only when severe plastic deformations are involved (machining). Consequently, the anisotropy was considered where the material presents plastic behaviour. During the cooling step the material behaviour depends mostly on the elastic properties. In particular, the Young's Modulus is responsible for the material components interaction. The anisotropy, responsible for the different mechanical behaviour in different directions, could also affect the Young's Modulus which could have different trend and value along the axial and hoop directions.

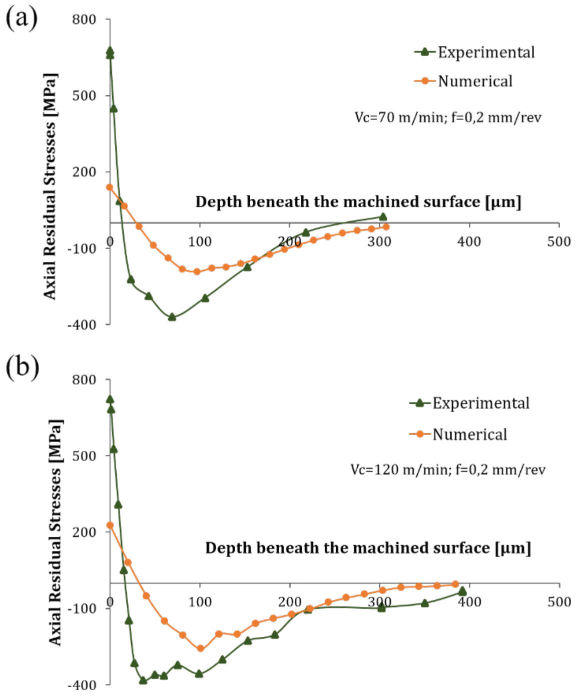

Fig. 6. Comparison of Residual Stress in Axial Direction for (a) #Test1, Vc=70m/min and f=0.2mm/rev; (b) #Test2, Vc=120m/min and f=0.2mm/rev.

4. Conclusion

A new constitutive model that takes into account the anisotropic mechanical behaviour of IN718 produced via AM was implemented to predict the residual stresses induced by the machining process. The model includes the effects of the dendritic microstructure, strain rate and temperature on the material plasticity flow stress. The residual stresses, hoop and axial direction were predicted and the numerical trends were compared with the experimental ones. The obtained results showed that the new model was able to estimate, along the hoop and axial directions, and the residual stresses (compressive stresses) beneath the machined surface and in particular below 100µm. The accuracy of the model was weak between 0µm and 100µm and this is mainly due to the combined effect of the elastic modulus and not optimised number of elements used. However, the numerical trends were successfully predicted and they are comparable with the experimental results. In conclusion, the constitutive model used to describe a material manufactured via AM resulted to be reliable in this first attempt to predict the residual stresses. Although, the first microns of the machined material did not show an accurate prediction of the residual stress, the model represents a first approach in simulating the machining of a material manufactured by AM. In particular, the model represents a starting point for a future machining modelling on AM materials and the influence of the machining parameters on the main features of process and surface quality.

Future developments will be devoted to the improvement of the existing model. Mesh optimisation will be essential in order to ensure the best correlation between experimental and numerical data. In fact, the introduction of optimised mesh size used in the sub-surface layers would drastically reduce the errors observed in the residual stress computation. Furthermore, the use of an elastic modulus that takes into account the anisotropy of the material considering its elastic behaviour would improve the prediction of the trend within the region characterised only by compressive stresses.

Reference

[1] Pollock TM, Tin S. Nickel-based superalloys for advanced turbine engines: Chemistry, microstructure, and properties. J Propuls Power 2006;22:361–74.

[2] Reed RC, Rae CMF. Physical Metallurgy of the Nickel-Based Superalloys. Phys. Metall. Fifth Ed., vol. 1, Elsevier Inc.; 2014, p. 2215–90.

[3] Akca E, Gürsel A. A Review on Superalloys and IN718 Nickel-Based INCONEL Superalloy. Period Eng Nat Sci 2015;3.

[4] Flynn JM, Shokrani A, Newman ST, Dhokia V. Hybrid additive and subtractive machine tools - Research and industrial developments. Int J Mach Tools Manuf 2016;101:79–101.

[5] Dudzinski D, Devillez A, Moufki A, Larrouquère D, Zerrouki V, Vigneau J. A review of developments towards dry and high speed machining of Inconel 718 alloy. Int J Mach Tools Manuf 2004;44:439–56.

[6] Wang X, Gong X, Chou K. Review on powder-bed laser additive manufacturing of Inconel 718 parts. Proc Inst Mech Eng Part B J Eng Manuf 2017;231:1890–903.

[7] Rotella G, Imbrogno S, Candamano S, Umbrello D. Surface integrity of machined additively manufactured Ti alloys. J Mater Process Technol 2018;259:180–5.
[8] Kaynak Y, Tascioglu E. Finish machining-induced surface roughness, microhardness and XRD analysis of selective laser melted Inconel 718 alloy. Procedia CIRP, vol. 71, Elsevier B.V.; 2018, p. 500–4.
[9] Calleja A, Urbikain G, González H, Cerrillo I, Polvorosa R, Lamikiz A. Inconel®718 superalloy machinability evaluation after laser cladding additive manufacturing process. Int J Adv Manuf Technol 2018;97:2873–85.
[10] Ulutan D, Ozel T. Machining induced surface integrity in titanium and nickel alloys: A review. Int J Mach Tools Manuf 2011;51:250–80.
[11] Lauro CH, Brandão LC, Ribeiro Filho SLM, Valente RAF, Davim JP. Finite Element Method in Machining Processes: A Review, Springer, Cham; 2015, p. 65–97.
[12] Özel T, Ulutan D. Prediction of machining induced residual stresses in turning of titanium and nickel based alloys with experiments and finite element simulations. CIRP Ann - Manuf Technol 2012;61:547–50.
[13] Arrazola PJ, Kortabarria A, Madariaga A, Esnaola JA, Fernandez E, Cappellini C, et al. On the machining induced residual stresses in IN718 nickel-based alloy: Experiments and predictions with finite element simulation. Simul Model Pract Theory 2014;41:87–103.
[14] Da Silva FAV, Denguir LA, Outeiro JC. Residual stresses prediction in machining of Inconel 718 superalloy using a constitutive model considering the state of stress. Procedia CIRP, vol. 87, Elsevier B.V.; 2020, p. 527–32.
[15] Yuan K, Guo W, Li P, Zhang Y, Li X, Lin X. Thermomechanical behavior of laser metal deposited Inconel 718 superalloy over a wide range of temperature and strain rate: Testing and constitutive modeling. Mech Mater 2019;135:13–25.
[16] International A. ASTM F3055-14a, Standard Specification for Additive Manufacturing Nickel Alloy (UNS N07718) with Powder Bed Fusion, ASTM International, West Conshocken, PA, 2014. ASTM Stand 2014:1–8.
[17] Tucho WM, Cuvillier P, Sjolyst-Kverneland A, Hansen V. Microstructure and hardness studies of Inconel 718 manufactured by selective laser melting before and after solution heat treatment. Mater Sci Eng A 2017;689:220–32.
[18] Ding RG, Huang ZW, Li HY, Mitchell I, Baxter G, Bowen P. Electron microscopy study of direct laser deposited IN718. Mater Charact 2015;106:324–37.
[19] Shamsaei N, Yadollahi A, Bian L, Thompson SM. An overview of Direct Laser Deposition for additive manufacturing; Part II: Mechanical behavior, process parameter optimization and control. Addit Manuf 2015;8:12–35.
[20] Noyan IC, Cohen JB. Residual Stress - Measurement by Diffraction and Interpretation. 1st Ed. Springer-Verlag New York; 1987.
[21] Careri F, Imbrogno S, Umbrello D, Attallah MM, Outeiro J, Batista AC. Machining and heat treatment as post-processing strategies for Ni-superalloys structures fabricated using direct energy deposition. J Manuf Process 2021;61:236–44.
[22] Careri F, Imbrogno S, Attallah MM, Essa K, Umbrello D. Finite element modeling of machining nickel superalloy produced by direct energy deposition process. Procedia Manuf., vol. 47, Elsevier B.V.; 2020, p. 525–9.
[23] Torrano I, Barbero O, Kortabarria A, Arrazola PJ. Prediction of residual stresses in turning of inconel 718. Adv. Mater. Res., vol. 223, Trans Tech Publications Ltd; 2011, p. 421–30. https://doi.org/10.4028/www.scientific.net/AMR.223.421.
[24] Outeiro JC, Umbrello D, M'Saoubi R, Jawahir I. Evaluation of present numerical models for predicting metal cutting performance and residual stresses. Mach Sci Technol 2015;19:183–216.